NACA

RESEARCH MEMORANDUM

DETERMINATION OF AVERAGE HEAT-TRANSFER COEFFICIENTS FOR A

CASCADE OF SYMMETRICAL IMPULSE TURBINE BLADES

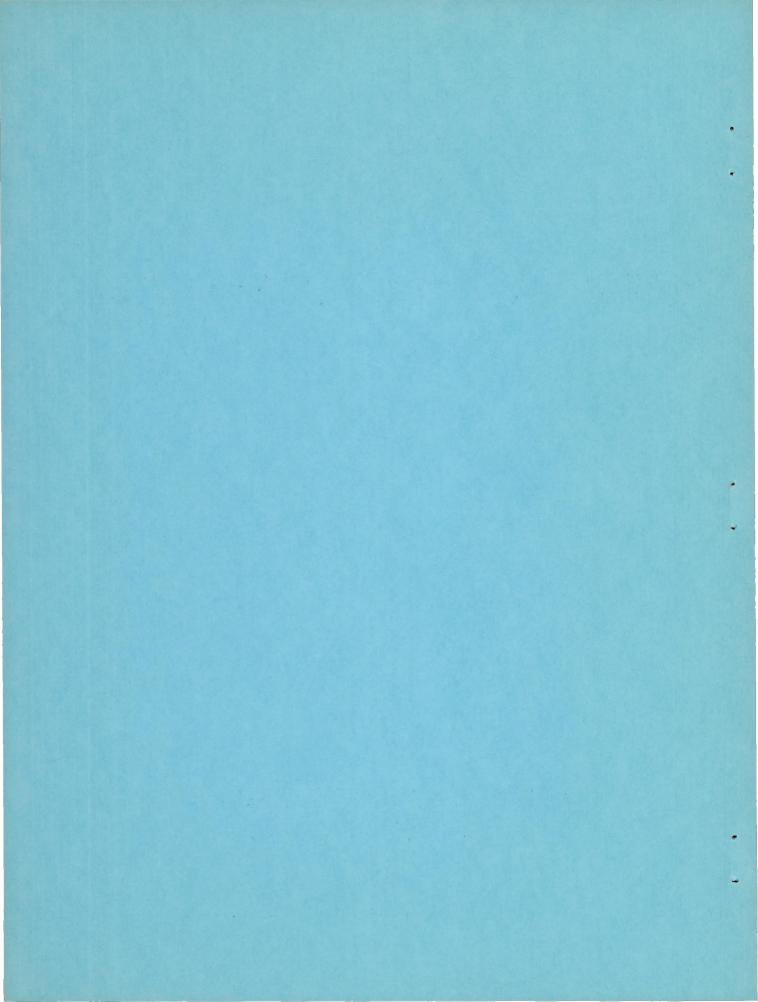I - HEAT TRANSFER FROM BLADES TO COLD AIR

By Gene L. Meyer

Lewis Flight Propulsion Laboratory
Cleveland, Ohio

NATIONAL ADVISORY COMMITTEE
FOR AERONAUTICS
WASHINGTON

November 10, 1948

NATIONAL ADVISORY COMMITTEE FOR AERONAUTICS

RESEARCH MEMORANDUM

DETERMINATION OF AVERAGE HEAT-TRANSFER COEFFICIENTS FOR A

CASCADE OF SYMMETRICAL IMPULSE TURBINE BLADES

I - HEAT TRANSFER FROM BLADES TO COLD AIR

By Gene L. Meyer

SUMMARY

Results of an investigation to determine average outside surface heat-transfer coefficients for a cascade of symmetrical impulse turbine blades are given. It has been theoretically shown that the effectiveness of both direct and indirect turbine-blade cooling methods depends to a great extent on the value of the heat-transfer coefficient between the gases and the blades. Because of the lack of data necessary to establish fundamental heat-transfer laws applicable to turbine blades, the NACA has started a comprehensive program that will meet these needs. As a part of this program, the heat transfer in a cascade of rim-cooled symmetrical impulse turbine blades was investigated. The blades were heated at the roots and cold air was exhausted past them. Adiabatic tests were first made to determine the thermal recovery factor for the blade, so that the heat-transfer coefficients could be based on the difference between the blade and effective gas temperatures.

The recovery factor was found to vary only slightly (from 0.78 to 0.89) with an exit Mach number ranging from 0.3 to 1.0 and was independent of the Reynolds number. The Nusselt number based on the effective gas temperature was independent of the Mach number in a range from 0.3 to 1.0. The results of the heat-transfer tests can be represented within ±10 percent by

$$Nu = 0.14 \ (Re)_i^{0.68} \ (Pr)^{1/3}$$

where Nu is Nusselt number, Re is Reynolds number, and Pr is Prandtl number. The characteristic dimension is arbitrarily taken as the blade perimeter divided by π and the inlet Reynolds number is used. This equation expresses equally well the results of investigations made by the General Electric Company on a cascade

of impulse blades five times the size of the NACA blades. No effect
due to the difference in curvature of the two blades was evident.
The results of the low-temperature runs are shown to be applicable
to the prediction of the effectiveness of rim cooling at elevated
temperatures for the blades used.

INTRODUCTION

Cooling methods for gas turbines can ordinarily be classified
as either indirect or direct. With the indirect method a coolant
is applied to the blade root or the tip, the rest of the blade
being cooled by conduction; with the direct method, a coolant is
forced through passages in the blade. Results of theoretical
analyses made at the NACA Cleveland laboratory (references 1 to 3)
to investigate both types of cooling indicate that the amount as
well as the effectiveness of the cooling depends to a great extent
on the convection heat-transfer coefficient between the hot gases
and the blades.

With indirect methods, the cooling effectiveness, as measured
by the allowable increase in effective gas temperature, increases
with a decrease in the heat-transfer coefficient. With direct
cooling, the dependence of the cooling effectiveness on the heat-
transfer coefficient is more complex, involving the ratio of the
coefficient on the hot-gas side to that on the coolant side. How-
ever, the same general trend as that for indirect cooling applies.
It is then clear that accurate cooling calculations for either
direct or indirect methods depend upon knowledge of the heat-
transfer laws between the gases and the blades.

Although a great deal of heat-transfer data is available on
the flow of fluids past plates, cylinders, and airfoils, none has
been published on turbine blades. The General Electric Company,
however, ran tests on a turbine-blade cascade using room-air-
and steam-heated hollow blades and obtained

$$Nu = 0.14 \ (Re)^{0.68} \ (Pr)^{1/3}$$

where

Nu   Nusselt number, based on blade perimeter divided by π

Re   Reynolds number, based on blade perimeter divided by π

Pr   Prandtl number

The temperature at which the air properties were taken was not given; however, the temperature range involved was so small that either the bulk or film temperature could be used without appreciably changing the results. It was recognized in this work that there might be an effect due to the reversal of heat flow, that is, heat transfer from the blade to the gas instead of from the gas to the blade, and a correction factor was applied. This correction, which was originally suggested for heating or cooling of fluids flowing through pipes, was estimated to have decreased Nu by only 3.4 percent. (The correction does not appear in the previous equation.) Similar work has undoubtedly been performed in other countries, but reports of the results are unavailable at present.

Because of the lack of correlated data necessary to establish fundamental heat-transfer laws applicable to turbine blades, a comprehensive program has been initiated at the NACA Cleveland laboratory that will meet these needs (reference 4). The problem is being experimentally attacked in two ways, by studying the heat transfer (a) in static turbine-blade cascades, and (b) in full-scale gas turbines. Cascades allow elaborate instrumentation, easy control of the factors involved in the convection and radiation processes, and rapid investigations of many blade configurations. The extremely large buoyancy forces due to rotation, which tend to increase free convection, and possible flow disturbances caused by the blades passing stationary nozzles are absent in cascades. The magnitude of these effects, though they are probably small, must be determined from research with actual turbines.

The over-all program of research on turbine cooling conducted at the Cleveland laboratory includes an investigation of the laws governing the heat transfer by convection between the gases surrounding a cascade of symmetrical impulse blades and the blades. The results obtained by using cold air as the fluid and by heating the blade roots are presented herein. Cold air, rather than hot gases, was used because its properties are well known, and there is no possibility of carbon deposits forming on the blades. By maintaining low blade temperatures, the influence of radiation was made negligible, and thus a fundamental relation for the convection heat transfer could be obtained. The blade temperature distribution was measured and the results were used in conjunction with a theory for the heat flow to compute the heat-transfer coefficient.

The purpose of this investigation is (a) to present for the blades tested a relation between the Nusselt and Reynolds numbers describing the heat transfer over a variation of inlet Reynolds numbers (based on the blade perimeter divided by π) of from 10,000 to 150,000 and a range of Mach numbers from 0.3 to 1.0, (b) to correlate and compare the results with those for other

turbine-blade cascades, cylinders, and streamlined bodies, and
(c) to apply the results to predict the effectiveness of rim cooling
by using the theory of reference 1.

THEORY

The general relation for forced-convection heat transfer is
often written in the dimensionless form

$$Nu = f(Re, Pr) = C(Re)^r(Pr)^s \tag{1}$$

where

Nu   Nusselt number, $\dfrac{h_c d}{k_g}$

h_c convection heat-transfer coefficient, (Btu/(hr)(sq ft)($^{\circ}$F))

d   characteristic dimension of body, (ft)

k_g thermal conductivity of gas, (Btu/(hr)(ft)($^{\circ}$F))

Re   Reynolds number, $\dfrac{V_g d \rho_g}{\mu_g}$

V_g gas velocity, (ft/sec)

ρ_g gas density, (slugs/cu ft)

μ_g gas viscosity, (slugs/ft-sec)

Pr   Prandtl number, $\dfrac{\mu_g c_{p,g}}{k_g}$

$c_{p,g}$ specific heat of gas at constant pressure, (Btu/(slug)($^{\circ}$F))

The symbols used in the analysis are defined in appendix A.

The Prandtl number can be considered a physical property for
a given gas and it varies only slightly with temperature. Thus the
geometrical shape does not affect it. For turbulent flow, the gas
properties μ_g, $c_{p,g}$, and k_g that are needed for Pr, Re,
and Nu are evaluated at the film temperature t_f, which is
assumed to be the mean of the average body temperature and the gas
static temperature. The characteristic dimension d for a turbine
blade is not immediately apparent and must be found by correlating

heat-transfer data for a number of different blades. The blade perimeter or perimeter divided by π has been commonly used. The heat-transfer coefficient is defined as the rate of heat transfer per unit area per unit temperature difference between the gas and the blade surface

$$h_c = \frac{Q}{S\Delta t} \tag{2}$$

where

Q   rate of heat transfer, (Btu/hr)

S   surface area, (sq ft)

Δt temperature difference between gas and blade surface, ($^\circ$F)

The value of Δt depends upon the method by which it is evaluated, as will be indicated.

The surface temperature is usually well defined and at low Mach numbers little difficulty is encountered in choosing a gas temperature because the static and total temperatures are very nearly equal. However, at high Mach numbers, these temperatures differ appreciably and different coefficients can be obtained, depending upon which temperature is used. Regardless of which temperature (total or static) is used, h_c may be positive or negative for the same direction of heat flow and a value of zero must be assumed for h_c for the adiabatic case.

In order to overcome these disadvantages, the heat-transfer coefficient is based on an effective gas temperature $t_{g,e}$, which is defined as the temperature a body assumes in the absence of heat transfer (the adiabatic body temperature). A coefficient based on this temperature is always positive and greater than zero. Furthermore, it has been shown to be independent of the Mach number and the temperature difference Δt. (See references 5 and 6.)

For any particular geometrical configuration, the effective gas temperature can be related to the total and static temperatures by a recovery factor α, defined by the equation

$$\alpha = \frac{t_{g,e} - t_{g,s}}{t_{g,t} - t_{g,s}} = \frac{t_{g,e} - t_{g,s}}{V_g^2/2Jc_{p,g}} \tag{3}$$

where

$t_{g,s}$ static temperature of gas, ($^\circ$F)

$t_{g,t}$ total temperature of gas, ($^\circ$F)

J   mechanical equivalent of heat, 778 (ft-lb/Btu)

In a theoretical study, Pohlhausen derived an expression for the recovery factor for flow past plates as a function of only the Prandtl number (reference 7). Numerous experiments have been performed with air flowing past plates, parallel to wires, normal to single cylinders, and inside cylindrical tubes to obtain recovery factors. (See bibliography listed on p. 4 of reference 5.) Results of these experiments indicate that there is only a small Reynolds number effect; the principal variable is the Mach number for a fixed Prandtl number. Eckert and Weise (reference 8) tested three shapes of turbine blades, for which they determined α. They found some variation with blade shape and Mach number, but made no mention of a Reynolds number effect.

In equation (2), it is seen that once α is known for a particular setup, Δt can be based on $t_{g,e}$ by use of equation (3), and it is only necessary to determine Q in order to find h_c. However, it was difficult to measure Q accurately in the test apparatus used and an alternate method of computing h_c was devised.

The one-dimensional temperature distribution for a turbine blade heated or cooled at the root can be found from a heat balance of the blade (appendix B). If radiation is neglected,

$$\theta = \theta_0 \frac{\cosh m (L - x)}{\cosh mL} \tag{4}$$

where

θ excess of blade temperature over effective gas temperature
       at blade position x, ($^\circ$F)

θ_0 excess of blade temperature at x = 0 (blade root) over
       effective gas temperature, ($^\circ$F)

$m = \sqrt{\dfrac{h_{c,b}\, b}{k_{m,a}\, A}}$, (ft^{-1})

L   distance from blade root to point at which $d\theta/dx$ is
         zero, (ft)

x   radial position on blade measured from the root, (ft)

$h_{c,b}$ convection heat-transfer coefficient from gas to blade,
         (Btu/(hr)(sq ft)($^\circ$F))

b   blade perimeter, (ft)

$k_{m,a}$ average thermal conductivity of blade material,(Btu/(hr)(ft)($^\circ$F))

A   cross-sectional area of blade, (sq ft)

The excess of the blade temperature over the effective gas tem-
perature θ is a function only of x, the quantities θ_0, L,
and m being constants for a given set of conditions. If the tem-
perature distribution is known, that is, θ as a function of x,
then θ_0 can be found by inspection, and m and L can be computed
by use of the method of least squares. Because

$$m = \sqrt{\frac{h_{c,b}\ b}{k_{m,a}\ A}}$$

the heat-transfer coefficient can ultimately be determined.

In deriving the expression for the temperature distribution
(equation (4)), the following assumptions are made:

1. The blade is of uniform cross-sectional area and perimeter
over the blade height.

2. The thermal conductivity of the blade metal, the average
heat-transfer coefficient, and the effective gas temperature are
constant over the blade height.

3. The temperature gradients in any cross section of the blade
perpendicular to the radius are negligible.

4. Radiation can be neglected.

5. At some position on the blade L, there is no heat flow
and $d\theta/dx = 0$.

It will be shown later that these assumptions are actually
experimental conditions in the setup used.

By using the experimental value of $h_{c,b}$, Nu can be computed based on an arbitrary dimension for d. The exponent of Pr in equation (1) has been found to have a value of approximately one-third for the flow of a gas around a body. The constants C and can be determined by plotting $Nu/(Pr)^{1/3}$ as a function of Re.

DESCRIPTION OF APPARATUS

The general arrangement of the apparatus is shown in figure 1. Refrigerated air, under a positive pressure (5 in. Hg), passed successively through a heater, a VDI orifice, a throttling valve, a calming section, an inlet nozzle, a test section, another throttling valve, and into the laboratory exhaust system. The air temperature could be held constant within ±0.5° F.

Details of the test section are shown in figures 2 and 3. The blades are made of Inconel and are of a symmetrical impulse design with a constant cross-sectional area and perimeter to conform to the first assumption of the temperature-distribution derivation; they are brazed to a bronze dummy-wheel section with a pitch-line radius of 5.50 inches. The blade solidity, defined as the ratio of the blade chord to the pitch, is 1.92. The blades are shrouded at the tip to form a flow passage 1 inch in height.

The blade assembly fits between a split Inconel nozzle block, only the exit half of which is shown in figure 3. The blade roots can be heated by conduction through the bronze wheel section. The heat is supplied by means of an electric furnace, the bronze protruding down into the furnace.

The temperature distribution of one blade is measured by means of a radiation-type thermocouple probe shown in figure 4 and described in appendix B. A hole, 1/16 inch in diameter, extended radially from tip to root through the center of one blade. A 1/16-inch-inside-diameter tube, which acts as a guide for the probe, is fitted flush with the blade tip so that the two holes are concentric. By moving the probe in the blade, the temperature at any point can be determined. Probe positions are measured with a calibrated screw accurate within ±0.001 inch. Calibrations of the probe (appendix C) insured the accuracy of the readings.

In order to check the validity of the assumption of a one-dimensional temperature distribution, fixed thermocouples were installed on three blades. Three thermocouples peened into 1/32-inch-diameter holes were in a plane perpendicular to the span of the blade

on each blade. The distances of the three planes from the tips are
0.23, 0.63, and 1.20 inches. Chordwise locations of these thermo-
couples are indicated by circles in figure 2.

Air inlet and exit total temperatures were measured in 6-inch
ducts immediately before and after the test section. These ducts
are large enough, compared to the test section, that the total tem-
perature can be read directly. The thermocouple probe and inlet
total temperature were read differentially on a potentiometer in
conjunction with a light-beam galvanometer. Inlet total pressure
was measured by means of a probe located at the nozzle throat.
Inlet static pressure was measured with wall taps. Exit total and
static pressures were measured with two fixed calibrated tubes placed
between two blades at their trailing edges, as shown in figures 1
and 2.

PROCEDURE

Adiabatic runs to measure the blade recovery factor as well as
heat-transfer runs were necessary in order to obtain heat-transfer
coefficients based on the effective gas temperature. In both kinds
of run, however, the same measurements were taken, namely, orifice
conditions, blade inlet and exit pressures and temperatures, and
the difference between the blade temperature and the inlet-gas
total temperature as a function of the probe position.

For the adiabatic tests, the air temperature was so adjusted
that the blades assumed room temperature, and thus heat losses were
minimized. The Reynolds number was held constant by holding the mass
flow fixed, while the Mach number was varied from 0.3 to 1.0 by
changing the pressure ratio across the test section. Runs were made
with three different Reynolds numbers.

For the heat-transfer runs, the blade roots were heated with
an electric furnace as previously described, and unheated air was
exhausted past the blades. Runs were made at: (a) fixed Reynolds
number, in which the Mach number was varied as in the adiabatic runs,
and (b) variable Reynolds and Mach number with a ten-fold range of
Reynolds number.

CALCULATION OF RESULTS

Adiabatic Runs

It is advantageous to write the recovery factor in the form

$$\alpha = 1 - \frac{t_{g,t} - t_{g,e}}{t_{g,t} - t_{g,s}} = 1 - \frac{t_{g,t} - t_{g,e}}{\dfrac{V_g^2}{2Jc_{p,g}}} \tag{5}$$

because the term $(t_{g,t} - t_{g,e})$ was experimentally measured, and in the adiabatic run the effective gas temperature was the average blade temperature. The gas velocity V_g is a function of the total-temperature and pressure ratio

$$V_g = \sqrt{\frac{2g\gamma R T_{g,t}}{\gamma-1} \left[1 - \left(\frac{p}{P}\right)^{\frac{\gamma-1}{\gamma}} \right]} \tag{6}$$

where

g   acceleration due to gravity, 32.17 (ft/sec^2)

γ ratio of specific heat at constant pressure to that at constant volume for air, 1.395

R   gas constant for air, 53.30 $(ft/^{O}R)$

$T_{g,t}$ total gas temperature, (^{O}R)

p   static gas pressure, (in. Hg)

P   total gas pressure, (in. Hg)

Because the total temperature was constant through the blade passage, either the inlet or exit velocity could be computed by equation (6), using the pressure ratio at that position.

Results of total- and static-pressure surveys indicated that whereas the velocity distribution was uniform at the blade inlet, separation was occurring at some point in the passage; therefore a velocity gradient resulted from inlet to exit. The small size of the blades made it impossible to determine at which point the separation took place. However, in analyzing the test data, it became

apparent that the conditions measured at the blade exit were controlling the thermal processes in the blades. Recovery factors were therefore computed using the exit velocity and correlated with the exit Mach number M_O

$$M_O = \sqrt{\frac{2}{\gamma-1}\left[\left(\frac{P}{p}\right)_O^{\frac{\gamma-1}{\gamma}} - 1\right]} \tag{7}$$

Heat-Transfer Runs

The average heat-transfer coefficient has been related to the blade-temperature distribution by equation (4). In order to check the theory experimentally, the test setup must agree with the assumptions upon which equation (4) is developed. These conditions were met in the following manner:

1. The blade was designed with a constant cross-section area and perimeter over its entire height.

2. The temperature differences from blade tip to root were kept small enough that thermal-conductivity variations were negligible, less than 7 percent. A comparison of a more exact derivation in which the thermal conductivity was considered a function of the temperature and equation (4) where the average conductivity for the temperature range was used resulted in a negligible difference. Even at greater temperature differences than those used in the experiments, the error could be neglected. A constant gas temperature was achieved by providing ample mixing length in the large duct before the test section and by the use of unheated air.

3. Fixed thermocouples in the blade, arranged to give a two-dimensional temperature distribution, indicated that gradients perpendicular to the radius could be neglected.

4. In order to minimize radiation effects, maximum blade temperatures were kept below 200° F. Because of the characteristics of the temperature distribution, over half the blade was at a temperature less than 100° F for all runs. The temperature of the blade surroundings varied between 50° and 75° F.

5. A point of zero heat flow was obtained by maintaining the gas temperature below that of the room. In effect then, the blade

was heated at the root by the furnace and at the tip by the room air because it assumed approximately the gas temperature at this zero heat-flow position.

The recovery factors found in the adiabatic runs were used to convert the measured temperature difference $t_m - t_{g,t}$ to one based on $t_{g,e}$ as follows:

For a given M_o, found from equation (7), a value of α was chosen. The exit velocity was computed by use of equation (6) by using the total and static pressures measured at the blade exit. From equation (5),

$$\theta \equiv (t_m - t_{g,e}) = (t_m - t_{g,t}) + (1 - \alpha)\frac{V_{g,o}{}^2}{2Jc_{p,g}}$$

where

t_m \qquad blade temperature, ($^\circ$F)

$V_{g,o}$ \qquad velocity of gas at exit, (ft/sec)

With θ known as a function of x, it was only necessary to determine the constants of equation (4) in order to determine h_c. However, to apply the method of least squares to a nonlinear equation, the observation equation (4) had to be transformed into a linear equation by expanding in a Taylor's series, neglecting all terms of powers higher than one (reference 9). The resulting observation equation took the form

$$\left(\frac{\partial \theta}{\partial m}\right) m' + \left(\frac{\partial \theta}{\partial L}\right) L' = \theta - \theta_l \tag{8}$$

where

m', L' \qquad corrections to approximate values of m and L found by least squares

θ_l \qquad value of θ computed from approximate m and L

For a given run, approximate values of m and L had to be assumed from which θ_l for each measured value of x was computed using equation (4). The results were substituted in equation (8) and the normal equations were formed and solved for m' and L'. The corrections were added to the assumed values to give the m and L that best fit the data points. When either correction,

m' and L', was large, the process was repeated until a negligible change occurred.

An approximate value of L was found by plotting the observed temperature distribution and picking the position at which $d\theta/dx$ was equal to zero. The value of L varied from run to run. Because

$$m = \sqrt{\frac{h_{c,b}}{k_{m,a}} \frac{b}{A}}$$

and b and A are known, only $h_{c,b}$ and $k_{m,a}$ must be assumed to find m. The blade thermal conductivity, based on experimental data for Inconel, was chosen for the integrated average blade temperature. The average heat-transfer coefficient can be written

$$h_{c,b} = \frac{Q}{b\int_0^L \theta \, dx} = \frac{-k_{m,0} \, A \left(\dfrac{d\theta}{dx}\right)_{x=0}}{b\int_0^L \theta \, dx} \tag{9}$$

where

$k_{m,0}$ thermal conductivity of the blade material for the temperature at x=0, (Btu/(hr)(ft)($^\circ$F))

$\left(\dfrac{d\theta}{dx}\right)_{x=0}$ temperature gradient at the point x=0, ($^\circ$F/ft)

The numerator of equation (9) is found by measuring the slope of the observed temperature-distribution curve at the position x=0, and multiplying by $-k_{m,0}$ A. The denominator is obtained from a graphical integration multiplied by b.

A typical temperature-distribution curve calculated from the theoretical equation obtained by least squares as compared to the observed data points is shown in figure 5.

The total temperature at the blades was assumed equal to the average of temperatures measured immediately before and after the test section. Reynolds numbers based on both blade inlet and exit conditions were calculated. Inlet Reynolds numbers $(Re)_1$ were computed by dividing the orifice mass flow by the flow area. The characteristic blade dimension was arbitrarily taken as the blade

perimeter divided by π. Exit Reynolds numbers $(Re)_o$ were based
on velocities and densities computed from conditions measured at the
blade outlets. The exit static temperature was computed from the
exit gas velocity using equation (6) and the exit pressure ratio.
Gas thermal conductivity, viscosity, and Prandtl number were evalu-
ated at the film temperature taken as the mean of the integrated
average blade and static (inlet or outlet) temperatures.

DISCUSSION OF RESULTS

Recovery factor. - The recovery factor for the blade investi-
gated is shown in figure 6 as a function of the exit Mach number.
The average adiabatic blade temperature was obtained by integrating
the local blade temperatures as measured by the thermocouple probe
and dividing by the blade length. Three sets of variable Mach
number runs were made, each at an approximately constant Re. The
exit Mach number was varied from 0.3 to 1.0, and the average exit
Reynolds numbers were 60,000, 120,000, and 132,000. The results of
all the runs lie about a single curve and there does not appear to
be an appreciable effect due to Re. For an exit Mach number range
from 0.3 to 1.0, α changes only from 0.78 to 0.89. Below
an M_o of 0.3, the temperature difference $(t_{g,t} - t_{g,e})$ became
too small to measure with precision. In this range, the effective
gas temperature can be assumed equal to the total gas temperature
without seriously changing results.

Also on figure 6 are shown some results taken from reference 8.
Two impulse blades, designated A and B were tested in a cascade
using air as the fluid. Blades A and B turned the air 128°
and 110°, respectively. Adiabatic blade temperatures were measured
with thermocouples at the thickest portion of the blade section.
However, it is not stated at what distance, say from the tip, the
measurements were made. If the blade temperature were constant from
tip to root, this omission would make no difference. However,
additional tests showed that heat was being lost from the blade ends
to the surrounding surfaces. The measured blade temperatures were
therefore probably somewhat low and, in turn, reduced α for the
blades. The Reynolds number range of the tests is not stated. Not-
withstanding these possible discrepancies, reasonably good agreement
was obtained between the tests reported herein and those of refer-
ence 8. The greatest deviation, which is for blade A, is less
than 10 percent.

Pohlhausen (reference 7) has theoretically shown that α is
a function of Pr and additional theory has indicated that this

function is $\sqrt{Pr}$. For these reasons, $\alpha/\sqrt{Pr}$ is also plotted against M_O in figure 6. Because all the data were obtained using air at room temperature, there is no relative displacement of the curves.

Heat-transfer coefficients. - The results of the heat-transfer tests are shown in the conventional manner, that is $Nu/(Pr)^{1/3}$ as a function of Re, in figure 7. The characteristic blade dimension is arbitrarily taken as the perimeter divided by π for Nu and Re. The results can be written in equation form as

$$Nu = 0.14 \ (Re)_i^{0.68} \ (Pr)^{1/3}$$

with an accuracy of ±10 percent. An inlet Reynolds number range from 10,000 to 150,000 and an exit Mach number range M_O from 0.3 to 1.0 are covered.

The inlet Reynolds number is obtained by dividing the mass flow measured with the orifice by the flow area, and corresponds to conditions at the blade inlet. If the exit conditions are used to define an exit Reynolds number, the dashed curve results, which is based on the maximum gas velocity through the cascade and the corresponding density. The slopes of the two curves are approximately equal, but $Nu/(Pr)^{1/3}$ based on exit conditions is lower by 13 percent and can be represented by

$$Nu = 0.21 \ (Re)_o^{0.63} \ (Pr)^{1/3}$$

with an accuracy within ±10 percent.

It was analytically shown (reference 6) that the Nusselt number based on the effective gas temperature is independent of the Mach number. Verification of this theory is given in figure 8. Results of three constant $(Re)_o$ runs in which M_O was varied are shown. Inasmuch as it was impossible to hold $(Re)_o$ absolutely fixed, $Nu/(Pr)^{1/3}$ was corrected for $(Re)_o$ variations from an average value for each run. The correction was applied by multiplying the observed $Nu/(Pr)^{1/3}$ by the ratio of the average $(Re)_o$ to the observed $(Re)_o$ raised to the 0.63 power. In general, the experimental scatter for these runs is no greater than that shown in figure 7. In all three cases, the maximum deviation from the mean value is ±10 percent and only ±5 percent for most of the points.

Effective gas temperature. - The use of heat-transfer coefficients based on the effective gas temperature is a refinement needed

only when the temperature differences involved are small, as was
the case for these tests. As a rather extreme example, consider a
blade at 105° F, the gas total temperature at 80° F, and a M_O
equal to 1.0. The ratio of $h_{c,b}$ based on $t_{g,t}$ to that based
on $t_{g,e}$ is 1.64. If the blade temperature is increased to 1080° F,
the ratio is reduced to 1.016. At higher gas-temperature levels,
the general trend is the same, although the percentage differences
increase.

COMPARISON OF RESULTS

Turbine cascades. - The results of this investigation are
compared with those of other forced-convection investigations in
figure 9. The cascade data of the General Electric Company coin-
cide perfectly with that of the NACA, based on $(Re)_i$. Because
General Electric based Re on the mass flow measured by an orifice,
the only proper basis of comparison would be $(Re)_i$, which is
obtained in a similar manner. Both blades were impulse; the blade
used by General Electric turned the air 134° and had a 3.08-inch
chord; the NACA blade turned the air 106° and had a 0.68-inch chord.
The solidity of the two cascades was the same. General Electric
Company also assumed an average recovery factor α equal to 0.85
for all runs.

Notwithstanding the differences in curvature and size of the
two blades, an excellent correlation was obtained by using the
blade perimeter divided by π as the characteristic dimension.
Of course, the blade perimeter or any constant times the perimeter
could have been used equally well. No effect due to the amount of
blade curvature was present insofar as these two investigations
reveal. It is quite probable that separation occurred at about
the same point in each cascade and thus similar flow was established.
By investigating blades of smaller curvature than those used in
these runs, that is, blades in which separation is delayed or
eliminated, some effects of the curvature might be found.

When differences in shape involve more than merely the amount
of curvature, such as a reaction blade compared with an impulse
blade, it seems unlikely that data will be correlated by only a
blade dimension.

Because convection heat transfer is a boundary-layer phenomenon,
there is some likelihood that data of different blades will never be
correlated by the simple means outlined. Possibly, only through

theoretical boundary-layer studies that take into account the veloc-
ity distribution about the blade will methods be developed to calcu-
late heat-transfer coefficients for an arbitrary shape. Another
promising mode of attack is by use of Reynolds' analogy, which considers
the similarity between heat transfer and momentum transfer. Whereas
neither of these approaches is likely to be simple, they will be
much more satisfactory than experimental determinations for every
blade shape.

Cylinders and streamline bodies. - The data for air flowing
normal to single cylinders and streamline bodies (reference 10) are
also shown in figure 9. Again, the slopes for all the curves are
approximately equal, but the magnitudes of $Nu/(Pr)^{1/3}$ differ. Values
for single cylinders and those for streamline bodies are 20 percent
and 10 percent lower than those for the NACA blades based on $(Re)_i$,
respectively.

Application to rim-cooling theory. - In addition to the cold-
air tests, a high-temperature run with hot gases was made. The
results of the cold-air runs are used to predict the cooling
effectiveness of the NACA blades for this run.

The effectiveness of rim cooling defined in reference 1 is
measured by the allowable increase in effective gas temperature as
limited by the blade stresses. For a fixed blade life, speed, and
amount of cooling, the effectiveness is a function of only the
quantity mL. The value of mL will now be predicted from the flow
conditions and compared with the test value for a high-temperature
run.

The experimental conditions are:

Excess of blade temperature at root over effective
  gas temperature, $^\circ$F . . . . -452
Inlet Reynolds number 49,600
Average blade thermal conductivity, Btu/(hr)(ft)($^\circ$F). 19.7
Blade length, ft 0.1042
Effective gas temperature, $^\circ$F 1167
Film temperature, $^\circ$F 1000
Gas thermal conductivity, Btu/(hr)(ft)($^\circ$F). 0.036
Prandtl number 0.65
Blade perimeter divided by π, ft 0.0473

From figure 7,

$$\frac{Nu}{(Pr)^{1/3}} = 211$$

$$h_{c,b} = 139 (Btu/(hr)(sq\ ft)(^{o}F))$$

and

$$m = 43.4\ ft^{-1}$$

The geometrical blade length is taken as equal to L. The pre-
dicted value of mL is 4.53. From these values of m and L,
the temperature distribution can be calculated using equation (4).
The result is

$$\theta = -9.73 \cosh 43.4\ (0.1042 - x)$$

By using the experimental temperature distribution, the measured
value of mL can be obtained by applying the method of least
squares, as previously discussed. The value of mL thus obtained
is 4.26.

The allowable increase in effective gas temperature for the
two values of mL can be found from a cross plot of figure 6 in
reference 1. For a constant value of θ_0 equal to -452° F, the
following results are obtained:

	mL	$\Delta t_{g,e}$ (^{o}F)
Experimental	4.26	190
Predicted	4.53	183

The predicted value of $\Delta t_{g,e}$ is 4 percent lower than the
experimental value. Radiation effects are unaccounted for in the
predicted case. Also L is taken as the geometrical length of the
blade, whereas actually for this case it is slightly greater. In
spite of these approximations, good agreement is obtained. In fig-
ure 10, the predicted blade temperature distribution is compared
with the experimental results. The maximum error is only 10° F at
a blade temperature of 1047° F or 1.0 percent. The values of x
and L in figures 5 and 10 are given in inches to simplify the
curves.

SUMMARY OF RESULTS

From an investigation to determine average outside surface heat-transfer coefficients for a cascade of symmetrical impulse turbine blades, the following results were obtained:

1. For a range of inlet Reynolds numbers from 10,000 to 150,000 and exit Mach numbers of 0.3 to 1.0, the results of the heat-transfer tests can be represented within ±10 percent by

$$Nu = 0.14 \ (Re)_1^{0.68} \ (Pr)^{1/3}$$

where Nu is Nusselt number, $(Re)_1$ is Reynolds number at the inlet, and Pr is Prandtl number. The blade perimeter divided by π was used as the characteristic dimension in Nu and Re and the gas properties were evaluated at the average film temperature. The heat-transfer coefficient was based on the difference between the blade temperature and the effective gas temperature.

2. The preceding equation expresses equally well the result of cascade tests made by the General Electric Company on impulse blades five times the size of the NACA blade. No effect due to the difference in curvature of the two blades was apparent.

3. The effective gas temperature can be related to the total and static gas temperatures by a recovery factor, defined as the ratio of the difference between the effective and static gas temperatures to the difference between the total and static gas temperatures. It varied only slightly (from 0.78 to 0.89) with an exit Mach number ranging from 0.3 to 1.0 for the blade used and was independent of the Reynolds number.

4. The Nusselt number based on the difference between the blade and the effective gas temperature is independent of the Mach number up to a value of 1.0, at least.

CONCLUSIONS

From the preceding results, the following conclusions can be drawn:

1. The results of these low-temperature tests can be used to compute the effectiveness of rim cooling at elevated gas temperatures for the blades investigated.

2. Although a correlation was obtained between two blade cascades of different sizes by use of the blade perimeter divided by π as the characteristic dimension in the Reynolds and Nusselt numbers, it is not clear that this dimension will hold for all blade shapes and configurations. Additional experiments are necessary to add to the limited amount of experimental data now available.

Lewis Flight Propulsion Laboratory,
    National Advisory Committee for Aeronautics,
        Cleveland, Ohio.

APPENDIX A

SYMBOLS

The following symbols are used in this report:

A   area of blade cross section, sq ft

a   speed of sound, ft/sec

B   perimeter of thermocouple plug, ft

b   perimeter of blade section, ft

C_1, C_2
C_3, C_4 arbitrary constants

C, r, s   constants

c_p specific heat at constant pressure, Btu/(slug)($^{\circ}$F)

d   characteristic dimension in Reynolds and Nusselt numbers, ft

F   shape factor for radiation

g   acceleration due to gravity, 32.17 ft/sec^2

h_c convection heat-transfer coefficient, Btu/(hr)(sq ft)($^{\circ}$F)

$h_{c,b}$ convection heat-transfer coefficient from gas to blade,
             Btu/(hr)(sq ft)($^{\circ}$F)

J   mechanical equivalent of heat, 778 ft-lb/Btu

k   thermal conductivity, Btu/(hr)(ft)($^{\circ}$F)

L   distance from blade root to point at which $d\theta/dx$ is zero, ft

M   Mach number, V_g/a

m   rim-cooling parameter, $\sqrt{\dfrac{h_{c,b}\, b}{k_{m,a}\, A}}$, ft^{-1}

Nu   Nusselt number, $h_c d/k_g$

P   total pressure, in. Hg

p   static pressure, in. Hg

Pr   Prandtl number, $\dfrac{\mu_g \, c_{p,g}}{k_g}$

Q   rate of heat transfer, Btu/hr

R   gas constant for air, 53.30 ft-lb/(lb)(^{o}R)

Re   Reynolds number, $\dfrac{V_g \, d \, \rho_g}{\mu_g}$

S   surface area, sq ft

T   temperature, ^{o}R

t   temperature, ^{o}F

V   velocity, ft/sec

x   radial position on blade measured from root, ft

α thermal recovery factor relating effective, static, and
            total gas temperatures

β = $\sqrt{\dfrac{4\sigma \, BFT_a^{\,3}}{k_p \, A_p}}$, ft^{-1}

γ ratio of specific heat of air at constant pressure to that
            at constant volume, 1.395

Δt temperature difference between gas and blade surface, ^{o}F

$\Delta t_{g,e}$ allowable increase in effective gas temperature due to rim
            cooling, ^{o}F

θ excess blade temperature over effective gas temperature at
            blade position x, $(t_m - t_{g,e})$, ^{o}F

μ viscosity, slugs/ft-sec

ρ density, slugs/cu ft

σ Stefan-Boltzmann constant, Btu/(hr)(sq ft)(^{o}R)

φ $\dfrac{\theta_0}{\cosh mL}$, ^{o}R

Subscripts:

av   average

b   blade

c   convection

e   effective

f   film

g   gas

i   inlet

l value calculated for least-squares computations

m   blade metal

o   exit

p   plug of thermocouple probe

r   radiation

s   static

t   total

0   blade root $(x=0)$

1   upper surface of probe plug

2   lower surface of probe plug

Primed symbols indicate corrections to assumed values found by least squares.

APPENDIX B

DERIVATION OF ONE-DIMENSIONAL TEMPERATURE DISTRIBUTION

A steady-state heat balance for a differential element dx between two planes perpendicular to the blade length and at a distance x and x + dx from the blade root will be assumed. The difference between the amount of heat entering the element by conduction dQ_x and the amount leaving by conduction $dQ_{(x + dx)}$ is equal to the heat leaving by convection dQ_c if radiation can be neglected:

$$dQ_x - dQ(x + dx) = dQ_c \qquad \text{(B1)}$$

$$\left(-k_m A \frac{dt_m}{dx}\right) - \left(-k_m A \frac{dt_m}{dx} - k_m A \frac{d^2 t_m}{dx^2}\, dx\right) = h_{c,b}\, b (t_m - t_{g,e})\, dx \qquad \text{(B2)}$$

If

$$\frac{h_{c,b}\, b}{k_{m,a}\, A} = m^2$$

and $(t_m - t_{g,e})$ is set equal to θ, then because $t_{g,e}$ is constant,

$$\frac{d^2 t_m}{dx^2} = \frac{d^2 \theta}{dx^2}$$

Equation (B2) becomes

$$\frac{d^2 \theta}{dx^2} = m^2 \theta$$

A solution of this equation is

$$\theta = C_1 \cosh m\, (C_2 - x) \qquad \text{(B3)}$$

It is assumed that at some position on the blade L, $d\theta/dx = 0$. (For most actual turbine installations, L is closely equal to the geometrical blade length.) At $x = 0$, $\theta = \theta_0$.

Substitution of these boundary conditions in equation (B3) gives the final equation for the temperature distribution when radiation is neglected

$$\theta = \theta_0\, \frac{\cosh m\, (L - x)}{\cosh mL} \qquad \text{(B4)}$$

APPENDIX C

THERMOCOUPLE PROBE

The radiation-type thermocouple probe used to obtain the blade temperature distribution is shown in figure 4. A junction is formed by spot-welding 36-gage chromel-alumel wire to a small Inconel plug 0.055 inch in diameter and 0.032 inch high. The wires are insulated by two-hole Alundum tubing that has a 0.032-inch outside diameter and extends to within 1/2 inch of the Inconel plug. The gap is necessary to reduce the transfer of heat by conduction between the plug and the tubing. For mechanical strength, an Inconel tube is cemented around the upper portion of the Alundum tubing.

Before experimentally calibrating the probe, the effects of plug dimensions and material, that is, plug height and thermal conductivity, on the indicated temperature were theoretically investigated. Because the probe fits snugly into only a 1/16-inch-diameter hole, it was assumed that all the heat transfer between the walls and the plug and wires occurred by radiation.

The derivation of the temperature distribution in the thermocouple probe plug will now be indicated. (See fig. 11.) A steady-state heat balance for a differential element dx on the plug between two planes perpendicular to the blade length at a distance x and $x + dx$ from the blade root is assumed. The difference between the amount of heat entering the element by conduction dQ_x and the amount leaving by conduction $dQ_{(x + dx)}$ is equal to the heat leaving by radiation dQ_r; if convection can be neglected,

$$dQ_x - dQ_{(x + dx)} = dQ_r$$

$$-k_p A_p \frac{dT_p}{dx} - \left(-k_p A_p \frac{dT_p}{dx} - k_p A_p \frac{d^2 T_p}{dx^2} dx\right) = \sigma BF \left(T_m^4 - T_p^4\right) dx \tag{C1}$$

By expanding T^4 in a Taylor's series about an average temperature T_a and by using only the first two terms, the result is

$$T^4 = 4T_a^3 T - 3T_a^4 \tag{C2}$$

The wall temperature T_m can be written

$$T_m = T_{g,e} + \theta_0 \frac{\cosh m(L-x)}{\cosh mL}$$

Equation (Cl) becomes

$$k_p A_p \frac{d^2 T_p}{dx^2} = \sigma BF \left[4T_a^3 T_{g,e} + 4T_a^3 \theta_0 \frac{\cosh m(L-x)}{\cosh mL} - 4T_a^3 T_p \right] \qquad (C3)$$

$$\frac{d^2 T_p}{dx^2} = \beta^2 \left[T_{g,e} + \varphi \cosh m(L-x) - T_p \right] \qquad (C4)$$

A solution of equation (C4) is

$$T_p = T_{g,e} + C_3 e^{\beta x} + C_4 e^{-\beta x} + \frac{\beta^2 \varphi}{m^2 - \beta^2} \cosh m(L-x) \qquad (C5)$$

The constants C_3 and C_4 can be evaluated from the following boundary conditions:

(a) At the probe position

$$x = x_1$$

Measured at the top surface of the plug

$$T_p = T_{p,1}$$

where $T_{p,1}$ is the reading of the probe.

(b) Also at

$$x = x_1$$

$$Q_1 = -k_p A_p \left(\frac{dT_p}{dx} \right)_{x=x_1}$$

The amount of heat radiated to the plug surface at x_1 is computed by dividing the wall into layers and summing the total heat transfer, the radiation-shape factor for each position being taken into account. To this value is added the heat conducted through the thermocouple wires to give Q_1. This amount of heat can be computed by differentiating equation (C5) using the proper constants for the wire.

The reading of the probe $T_{p,1}$ is assumed for a given position and blade conditions. As outlined, all the constants of equation (C5) can be evaluated, and the heat transfer at the bottom of the plug at x_2 can then be calculated

$$Q_2 = -k_p A_p \left(\frac{dT_p}{dx}\right)_{x=x_2} \tag{C6}$$

The first term Q_2 can be calculated in the same manner as Q_1 omitting heat conduction through the wires. Values of $T_{p,1}$ are assumed until equation (C6) is satisfied.

From this type of calculation, it was concluded that: (a) The temperature drop through the plug was so small (less than 1° F) that the conductivity was of no importance and almost any material could be used; and (b) As the height of the plug was increased, the probe error increased. An optimum height of 0.032 inch was indicated.

With the results of the analysis serving as a guide, several probes were built and calibrated, as follows: A 1/16-inch-diameter hole was drilled from tip to root through the center of a blade. Five holes, each 1/32 inch in diameter, were drilled perpendicular to the original hole through the blade at different distances from the root. Thermocouples, 36-gage chromel-alumel, were inserted in the small holes so that they indicated the temperature at the surface of the 1/16-inch hole. A tube was soldered to the blade root through which cooling water was passed. The entire apparatus was placed in an electric furnace, and the readings of the probe compared with those of the fixed thermocouples. By varying the heat input, different gas temperatures could be simulated.

It was found that probes in which the plug height was greater than 0.032 inch read lower than the true temperature, as was indicated by the analysis. By using a plug height of 0.032 inch, very satisfactory agreement was obtained between the probe and the fixed thermocouples. The probe was very sensitive and attained thermal equilibrium quickly.

REFERENCES

1. Wolfenstein, Lincoln, Meyer, Gene L., and McCarthy, John S.:
   Cooling of Gas Turbines. II - Effectiveness of Rim Cooling of
   Blades. NACA RM No. E7B11b, 1947.

2. Brown, W. Byron, and Livingood, John N. B.: Cooling of Gas
   Turbines. III - Analysis of Rotor and Blade Temperatures in
   Liquid-Cooled Gas Turbines. NACA RM No. E7B11c, 1947.

3. Wolfenstein, Lincoln, Maxwell, Robert L., and McCarthy, John S.:
   Cooling of Gas Turbines. V - Effectiveness of Air Cooling of
   Hollow Blades. NACA RM No. E7B11e, 1947.

4. Ellerbrock, Herman H.: NACA Investigations of Gas Turbine Blade
   Cooling. Paper presented before I.A.S. (New York), Jan. 26, 1948.

5. McAdams, William H., Nicolai, Lloyd A., and Keenan, Joseph H.:
   Measurements of Recovery Factors and Coefficients of Heat
   Transfer in a Tube for Subsonic Flow of Air. NACA TN No. 985,
   1945.

6. Eckert, E., and Weise, W.: The Temperature of Unheated Bodies
   in a High-Speed Gas Stream. NACA TM No. 1000, 1941.

7. Pohlhausen, E.: Der Warmeaustausch zwischen festen Körpern und
   Flüssigkeiten mit kleiner Reibung und kleiner Wärmeleitung.
   Z.f.a.M.M., Bd. 1, Heft 2, 1921, S. 115-121.

8. Eckert, and Weise: The Temperature of Uncooled Turbine Blades
   in a Fast Stream of Gas. Reps. and Trans. No. 39, M.A.P.,
   June 26, 1946.

9. Merriman, Mansfield: Method of Least Squares. John Wiley & Sons,
   Inc., 8th ed., 1915, p. 200.

10. McAdams, William H.: Heat Transmission. McGraw-Hill Book Co.,
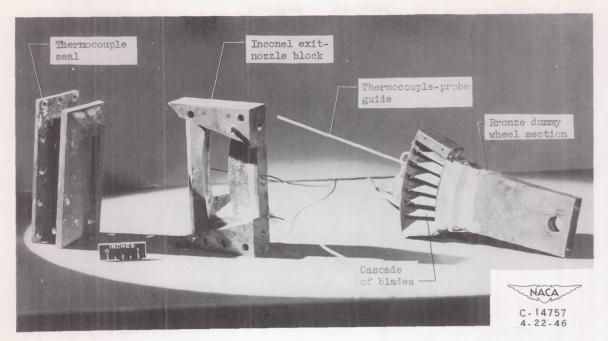   Inc., 2d ed., 1942, pp. 221, 236.

Exit-gas
thermocouple

Blade cascade

Thermocouple
probe

Inlet total-
and static-
pressure
tubes

Inlet nozzle

Inlet-gas
thermocouple

Calming section

Orifice static-
pressure-drop
tubes

Orifice air
thermocouple

Blade

Static-
pressure
tube

Total-
pressure
tube

Location of blade
exit pressure tubes

Inlet throttle
valve

Orifice

Air
heater

Air flow

To exhaust   Electric
furnace

NACA

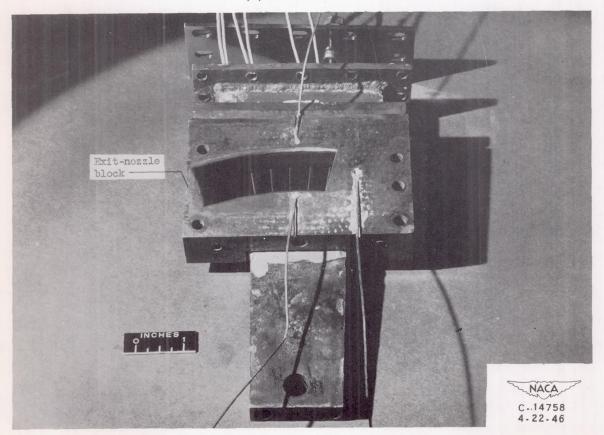Figure 1. - Experimental setup for rim-cooled turbine-blade cascade.

Figure 2. — Cross sections of symmetrical impulse
turbine blades.

Hydraulic radius, in.	0.092
Chord, in.	0.680
Perimeter, in.	1.785
Cross-sectional area, sq in.	0.0797
Pitch-line radius, in.	5.50
Number of blades in 360°	84
Solidity	1.92
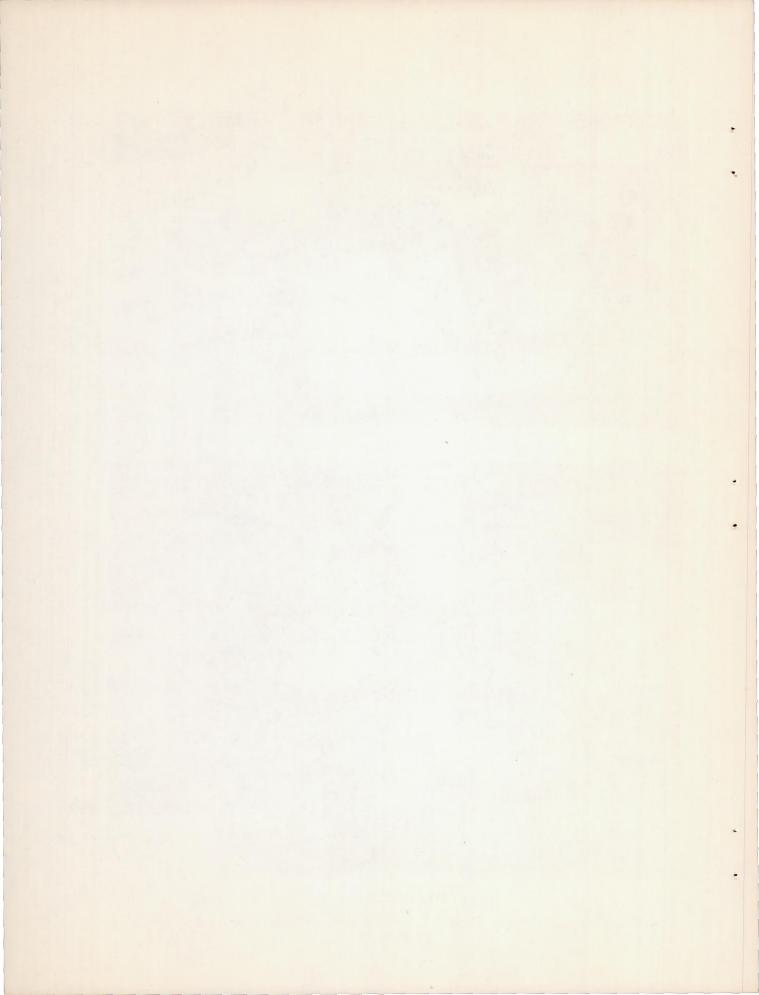
(a) Unassembled.

(b) Assembled.

Figure 3. - Special test rig for heat-transfer studies of symmetrical impulse turbine blades.
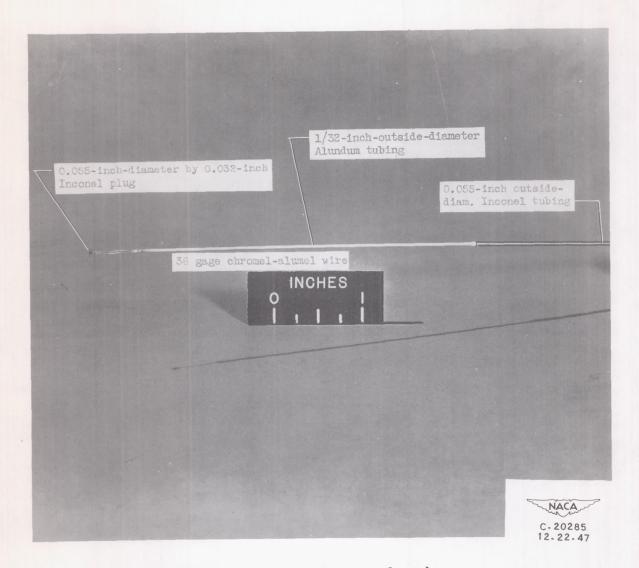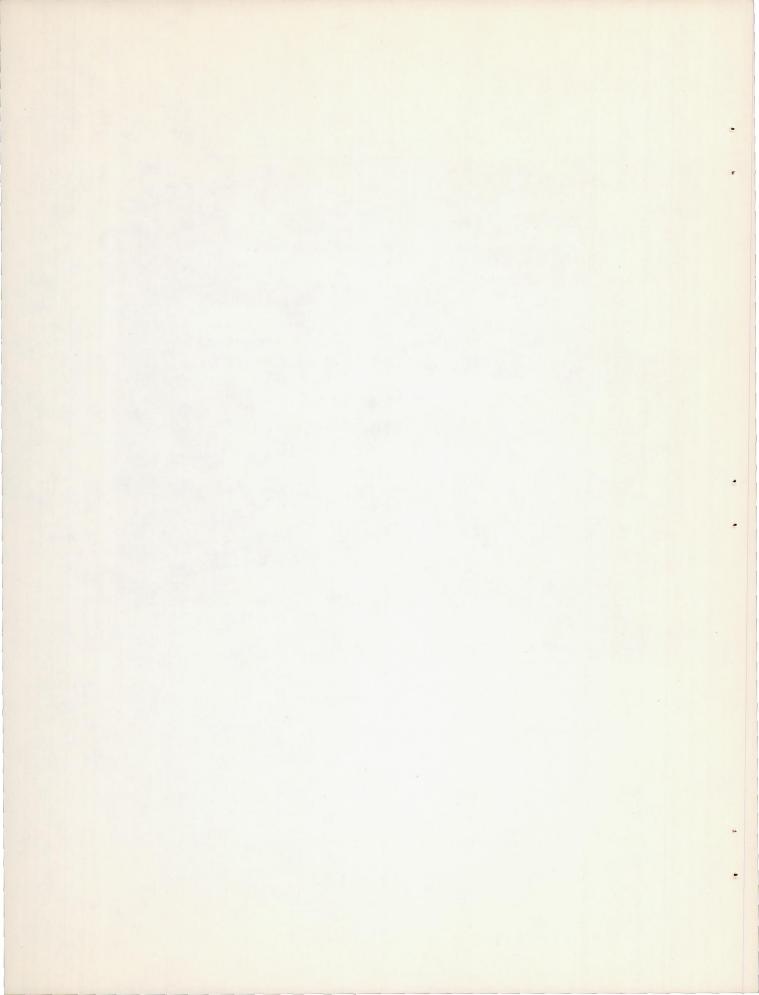
Figure 4. - Radiation-type thermocouple probe.
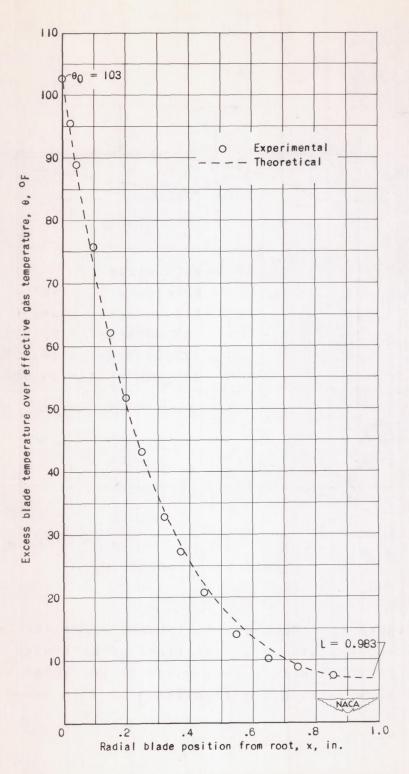
Figure 5. – Comparison of experimental blade temperature distribution and theoretical curve obtained by least squares. $\theta = 6.78 \cosh \dfrac{41.68 \, (0.983-x)}{12}$
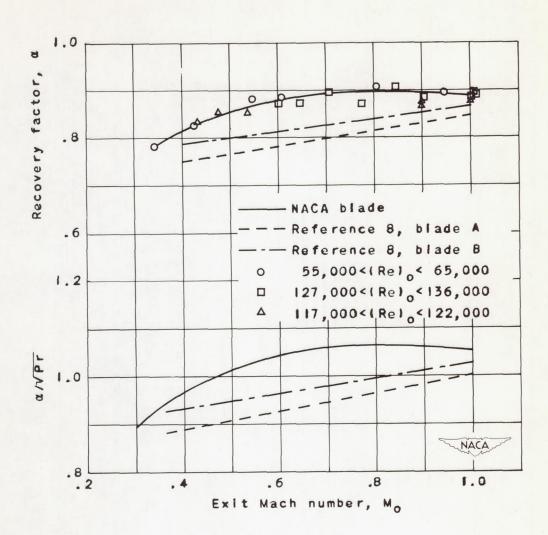
Figure 6. – Recovery factor and $\alpha/\sqrt{Pr}$ for impulse
turbine blades as functions of exit Mach number.
Exit Reynolds number based on perimeter divided
by π.   Gas properties taken at film temperature.

1013

Figure 7. – Correlation of heat-transfer data for air flowing past heated turbine blades. Pr, μ_g, k_g based on film temperature. Characteristic blade dimension equal to perimeter divided by π.
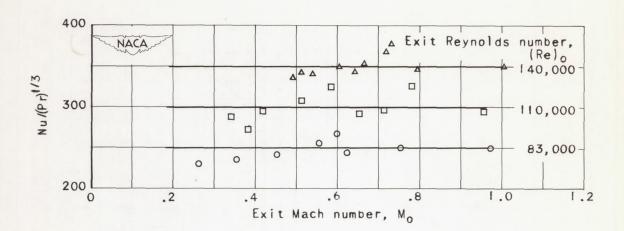
Figure 8. – Heat–transfer data for three constant exit Reynolds
numbers and variable exit Mach numbers. Characteristic blade
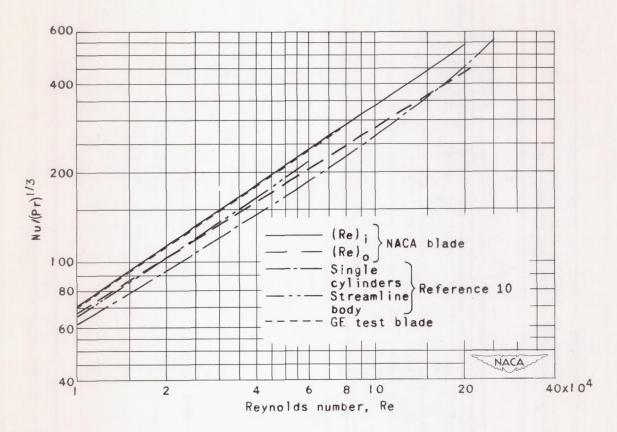dimension equal to perimeter divided by π. Gas properties
taken at film temperature.

1013

Figure 9. – Comparison of heat-transfer data for turbine-blade cascades, single cylinders, and streamline bodies. Reynolds and Nusselt numbers based on perimeter divided by π. Physical properties taken at film temperature.
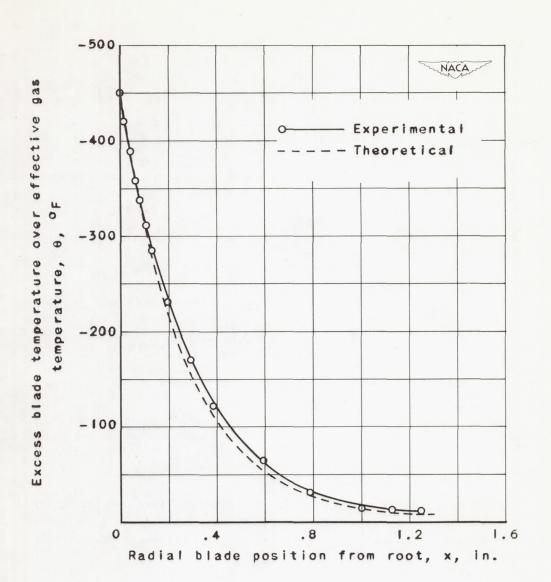
Figure 10. - Comparison of theoretical and experimental blade temperature distribution at effective gas temperature of 1167° F.

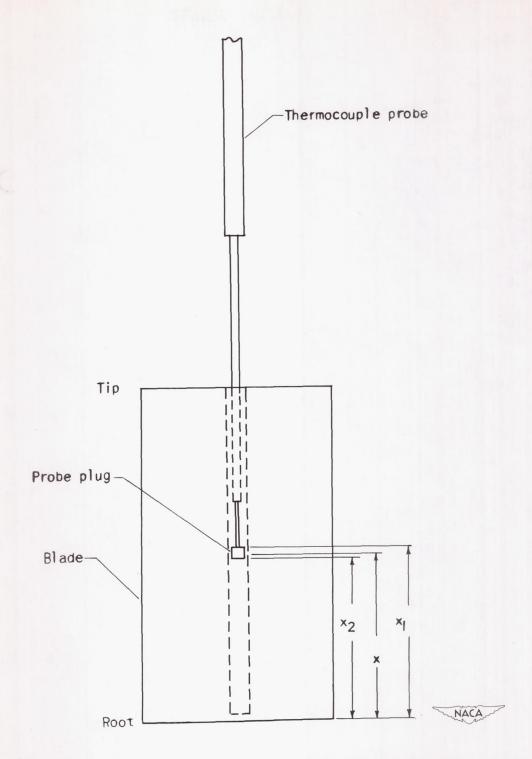$$\theta = -9.73 \cosh \frac{43.4 \ (1.25-x)}{12}$$

1013

Figure 11. – Coordinate system for radiation–
probe temperature-distribution analysis.